

# The deflection of a baroclinic jet by a wall in a rotating fluid

By J. A. WHITEHEAD

Woods Hole Oceanographic Institution, Woods Hole, Massachusetts 02543

(Received 8 May 1984 and in revised form 30 January 1985)

The momentum integral of a baroclinic jet of fluid in a rotating frame determines the relative size of two jets which are produced when the jet is split by a wall. Owing to lateral variation of velocity and depth of the jet, the percentage of fluid which goes to the right or left differs from that of the non-rotating jet, which is generally assumed to have no shear. For a northern hemisphere jet of zero or constant potential vorticity, much more fluid flows to the right than to the left; for a jet normal to the wall more than 65% goes to the right and less than 35% to the left.

## 1. Introduction

Some oceanic coastal currents comprise low-density water which, in the northern hemisphere, flows along the right-hand coast as one looks in the direction of current propagation. A good example is the Norwegian Coastal Current. This is principally fed by fresh water from the Baltic and it flows northward along the west coast of Norway. Other examples are the Greenland Current, which flows southward along the East Coast of Greenland and northward along the West Coast, and the Antarctic Coastal Current (an example of opposite rotation), which flows westward along the northern coast of Antarctica. There are many others. These currents contain low-density water by virtue of their low salinity from fresh water runoff from the land. They are separated from the deep oceanic water by a distinct front which comes to the surface at some distance offshore.

As a general problem in geophysical fluid dynamics, the jets and dynamics of the problem are strongly nonlinear since the front intersects the surface. The theoretical properties and behaviour of such currents have recently been studied. For analytical simplicity two classes of currents have been analysed; those with zero and those with constant potential vorticity. The simplest currents have zero potential vorticity. The assumption is that the current comes from a very deep upstream reservoir. Whitehead, Leetmaa & Knox (1974), Stern (1974), Bye & Whitehead (1975) and Shen (1981) investigated the control of this kind of current as it passed through a long rectangular channel (strait). Sambuco & Whitehead (1976) and Whitehead & Porter (1977) investigated the control of this kind of current by an axisymmetric sill and a very wide sill, respectively. They found that these geometries insure that the current has zero potential vorticity. Stern (1980) studied theoretically a current of zero potential vorticity when it had a nose as it moved next to a vertical wall, and Stern, Whitehead & Lien Hua (1982) extended the theoretical understanding of the speed and width of this current.

A more complicated current has constant potential vorticity. The assumption is that the current comes from a reservoir of constant depth. Analytical solutions have been found for these as well. Gill (1977), Nof (1978*a, b*) and Shen (1981) have

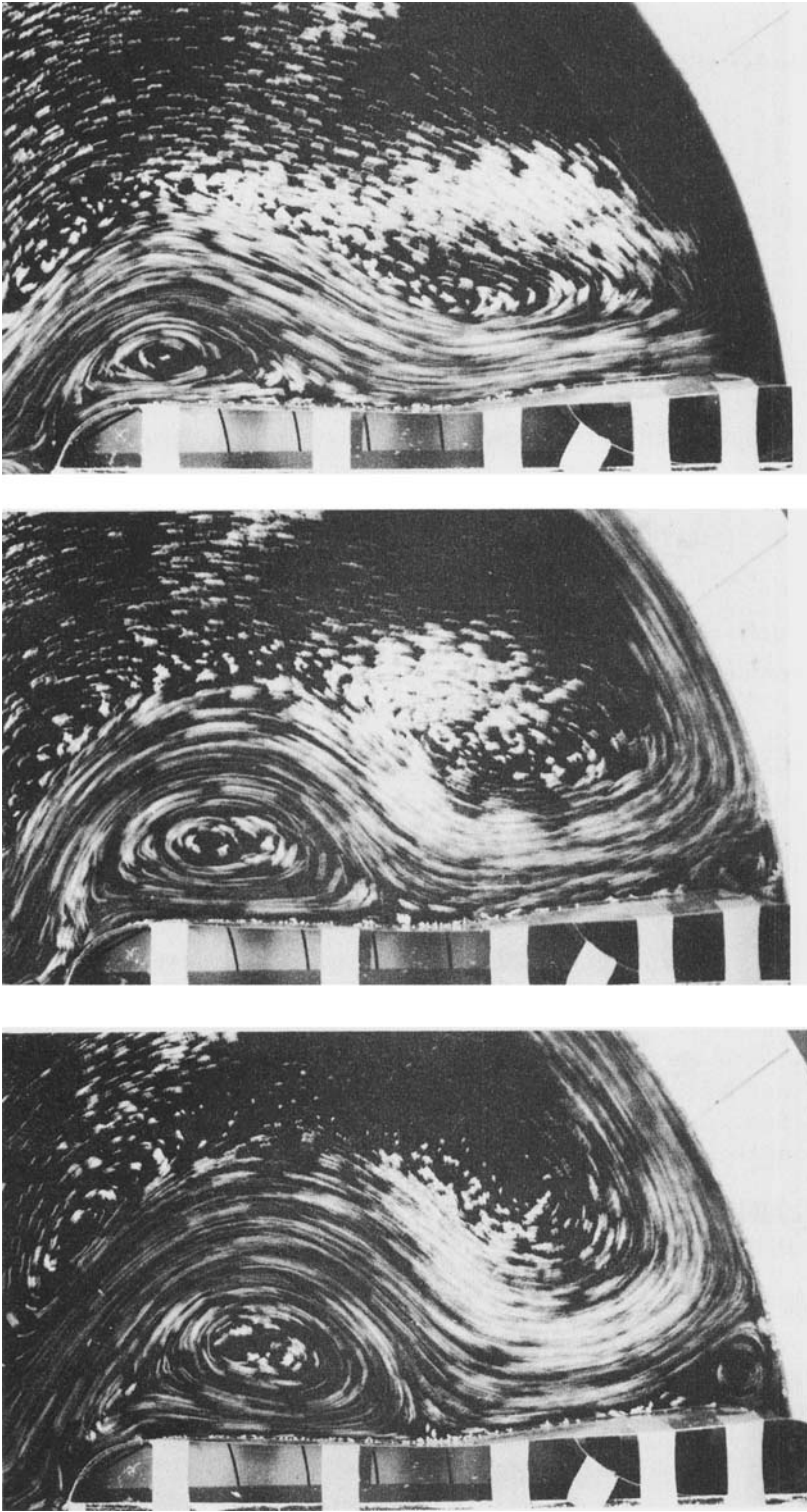


**FIGURE 1.** Sequence of streak photographs of an experimentally generated constant-potential-vorticity jet which separates from the wall and reimpinges on it, thus creating a stagnation point.

investigated the control of a current of constant potential vorticity by channels (straits) of various geometries. Griffiths & Linden (1981) and Killworth & Stern (1982) investigated the stability of axisymmetric gyres and wall currents of constant potential vorticity. Stern *et al.* (1982) studied a wall current when it had a nose, and Nof & Olson (1982) have investigated the movement of a jet of constant potential vorticity through a wall slot.

Many of the above studies report on laboratory experiments which duplicate these currents. In some there is a detachment of the current due to coastal irregularities, vorticity distribution in the current, or bottom topography, yet the reasons for detachment are ambiguous. There have been extensive laboratory observations of such detached jets by the Trondheim group (Ingebrigtsen 1979; Vinger & McClimans 1980; McClimans & Green 1983). In addition, a study of a free jet and a consequential gyre formation in the context of the Alboran Sea has been conducted by Whitehead & Miller (1979). In that case the free jet resulted from separation of the surface current from a curving wall. Figure 1 shows a sequence of photographs from the experiments. The free jet clearly reimpinges on the wall downstream of the separation point. The topic of this study is the behaviour of such a free jet as it impinges on a wall.

In the ocean, coastal currents sometimes leave the coast forever and are lost in the deep ocean, where they presumably break up into eddies which ultimately mix with the ocean. Sometimes, however, the current curves around and returns to the coast or intersects another coast. Good examples of this are the jet in the Alboran Sea impinging on the coast of Africa (Whitehead & Miller 1979) and the jet of water that emanates from the Tsugaru Strait north of Japan which comes back and hits the coast in conjunction with an eddy formation (Conlon 1981, 1982; Kawasaki & Sugimoto 1984). In cases where a jet hits the coast, it is important to determine what governs the splitting of the jet. Does it deflect to the left as it hits the coast and resume its flow in an unaltered state along the coast? Does it split up into two jets, one flowing to the left and another to the right? Does it reflect from the coast or does it even encounter difficulty in returning to a steady state?

All these questions are simply a subset of the general problem of the adjustment of a nonlinear jet in a rotating fluid as it impinges on a sidewall. In traditional hydrodynamics, well-known momentum balances govern nonlinear jets, as found in numerous text-books, for instance Prandtl & Tietjens (1957, p. 245). In geophysical fluid dynamics, the nonlinear jet in a two-layer rotating fluid has new, more complicated momentum balances, which will be derived for what seems to be the simplest class of nonlinear (i.e. those whose interface comes completely to the surface) baroclinic jets. These considerations lead to the prediction that a jet of zero or constant potential vorticity is partly deflected to the left (looking downstream) and partly to the right when it impinges onto a vertical wall. In no case does the fluid go completely to the left or to the right except for the extreme cases in which the jet just tangentially grazes the surface. An argument is advanced that this applies to a jet of any simple (i.e. one maximum) velocity distribution. Of course, all such distributions may not be stable. However, if the jet impinges onto a vertically sloping wall (or a coast), there could be an angle between the jet and the wall at which all fluid would go to the right or to the left. This is because a sloping coast can alter the velocity distribution of the jet, whereas a vertical wall cannot.

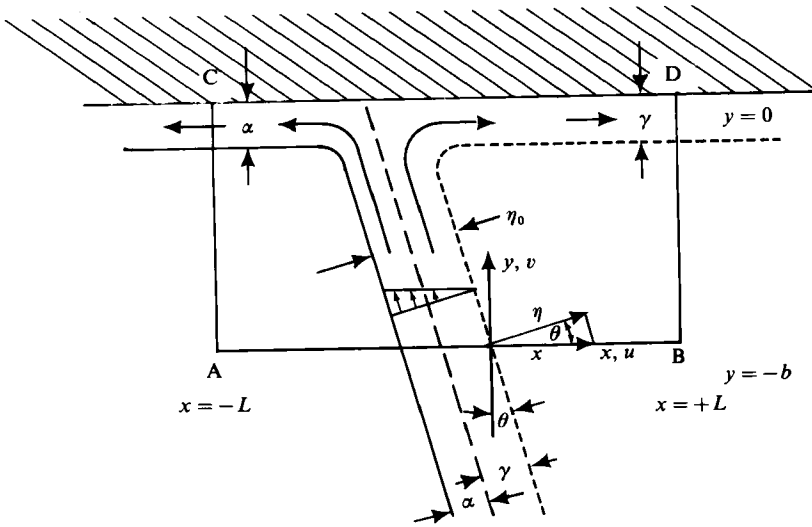


FIGURE 2. Top view of the problem. A jet of width  $\eta_0$  is coming into the control section through section AB and impinging upon the cross-hatched wall. It splits into two jets, one exiting at AC of width  $\alpha$ , the other exiting at BD of width  $\gamma$ . The incoming jet makes angle  $\theta$  with the normal to AB (which is parallel to CD). The fine dashed line is the 'inner' border of the jet, where the bottom of the jet reaches depth  $H$  and velocity becomes zero. It is adjacent to a stagnant fluid of depth  $H$ . The long dashed line is the stagnation point or 'dividing' streamline, whose position is unknown *ab initio*. The solid line is the edge of the 'front', where the jet interface intersects the surface. Sections of this are in figure 3.

2. A momentum integral

Consider the depth-averaged steady-state Navier–Stokes equations for a fluid of density  $\rho$  and depth  $h(x, y)$  lying over a motionless semi-infinite fluid of density  $\rho + \Delta\rho$  with  $\Delta\rho/\rho \ll 1$ :

$$(uh)_x + (vh)_y = 0, \tag{2.1a}$$

$$uu_x + vv_y - fv = -g'h_x, \tag{2.1b}$$

$$uv_x + vv_y + fu = -g'h_y, \tag{2.1c}$$

where  $g' = g \Delta\rho/\rho$ , and  $f = 2\Omega$  is the Coriolis parameter, where  $\Omega$  is the angular rate of rotation of the fluid.

From (2.1a), we can define a velocity potential

$$\psi_y = -uh, \tag{2.2a}$$

$$\psi_x = vh. \tag{2.2b}$$

Equations (2.1b) and (2.1c) can be multiplied by  $h$  in their steady state to read

$$huv_x + hvv_y - f\psi_x = -\frac{1}{2}g'(h^2)_x, \tag{2.3a}$$

$$huv_x + hvv_y - f\psi_y = -\frac{1}{2}g'(h^2)_y. \tag{2.3b}$$

Let us consider a situation in which a jet is impinging upon a coast from offshore, the jet having an angle  $\theta$  with the normal to the coast as shown in figure 2. The jet is purely baroclinic and a front separates dense fluid on the left and below from less dense fluid on the right and above. If  $\alpha$  is the width of the fluid which is going to the left, i.e. if it is the distance from the point of zero height to the stagnation-

point streamline, the task is to use the above equations to determine  $\alpha$ , and thence to estimate how much fluid flows to the left. The rest must flow to the right. A control volume is to be bounded by the coast at  $y = 0$ , by a left-hand boundary (AC) at  $x = -L$  and a right-hand boundary (BD) at  $x = +L$ , and by an offshore section (AB) at  $y = -b$  through which the current is introducing fluid from offshore. Equation (2.3a) can then be integrated in this control volume (in a manner similar to Nof & Olson 1983) as follows:

$$\int_{-b}^0 \int_{-L}^{+L} (huv_x + hvu_y - f\psi_x + \frac{1}{2}g'(h^2)_x) dx dy = 0. \tag{2.4a}$$

The two left-hand terms can be expanded so that (2.4a) reads

$$\int_{-b}^0 \int_{-L}^{+L} ((hu^2)_x - u(hu)_x + (huv)_y - u(hv)_y - f\psi_x + \frac{1}{2}g'(h^2)_x) dx dy = 0, \tag{2.4b}$$

and (2.1a) eliminates the second and fourth terms. Integrating the terms with total derivatives leads to

$$\int_{-b}^0 (hu^2 - f\psi + \frac{1}{2}g'h^2) dy \Big|_{x=-L}^{x=+L} + \int_{-L}^{+L} huv dx \Big|_{y=-b}^0 = 0. \tag{2.5}$$

It will be assumed that the currents are fully developed at the three open sides of the control volume, so velocity and height distributions are not changing in the direction of flow. This implies that

$$\frac{\partial}{\partial x}, v = 0 \quad \text{at } x = \pm L,$$

since the flow is along the wall. Then (2.3b) reads

$$(-f\psi = -\frac{1}{2}g'h^2)_y \quad \text{at } x = \pm L,$$

or

$$-f\psi + \frac{1}{2}g'h^2 = C, \text{ a constant.}$$

This is simply the geostrophic relation for a current flowing strictly in the  $\pm x$  direction. The stream function is arbitrary, but continuous everywhere and hence is the same at  $y = 0, x = \pm L$ . It follows that  $h$  is the same there as well in order to conserve volume flux, so we choose  $C = 0$  (other values of  $C$  do not change the problem, but complicate the algebra). Thus (2.5) reduces to the final momentum integral of the volume

$$\int_{-b}^0 hu^2 dy \Big|_{x=-L}^{x=+L} + \int_{-L}^{+L} huv dx \Big|_{y=-b}^0 = 0. \tag{2.6}$$

Because the flows are geostrophic owing to their lack of change in the direction of flow, the Coriolis-force terms have dropped out.

Equation (2.6) shows that effects of the rotation are not directly important. However, it is known and understood that rotation plays a large part in determining velocity and height profiles of the flows. One can analyse the two simplest types of jets – those with zero and those with constant potential vorticity.

Before proceeding, note that the balance in (2.6) leads to some obvious conclusions. Since there are only three terms, any situation in which one of the terms is zero must result in a balance between the other two. Thus if  $u = 0$  at  $y = -b$  (a current normal to the wall), the right-hand term of (2.6) is zero and the exit current must flow out at both  $x = \pm L$  to allow a balance between the two left-hand terms. If  $u = 0$  at  $+L$

or at  $-L$ , circumstances must be such that the velocity or depth profiles must be different between entrance and exit. Such circumstances may not always exist, as described in §3. If all three terms exist, we still can identify a relationship between incoming and outgoing flows. In situations where the jets encounter no bottom topography, the velocity and depth profiles are unchanged between entrance and exit. This allows calculations to be made as discussed in the following sections.

### 3. A zero-potential-vorticity jet

Potential vorticity is defined as  $(\nabla \times \mathbf{u} + f)/h$ , and it is conserved by any depth-averaged parcel of fluid. All progress to date in analysing nonlinear jets in rotating fluids has been made for jets of constant potential vorticity. The simplest cases have zero potential vorticity and can be produced in the laboratory or in nature in many ways. One very simple geometry, similar to that studied by Whitehead, Leetmaa & Knox (1974) and Whitehead (1985), consists of a deep reservoir of water with density  $\rho$  connected by a smoothed, much shallower passage to another deep reservoir of density  $\rho + \Delta\rho$ . If the passageway is initially blocked by a gate, and the gate is suddenly raised, a density current and counter current will start. The denser water will flow near the bottom and the less dense water will flow near the surface, but in an opposite direction. It is the latter current that we have in mind here. If the entrance between the deep ocean and the passage is sufficiently smooth, the columns of fluid will have undergone considerable shrinkage by the time they arrive at the passage. They will have almost zero potential vorticity [of size  $f(d_1/d_2)$ , where  $d_1$  is depth of the passage and  $d_2$  is the depth of the ocean]. The fluid will flow into the interior of the ocean of dense water as a zero-potential-vorticity jet. Such a jet is possibly a model of the Norwegian coastal current or the current of Atlantic water flowing into the Mediterranean, mentioned in the introduction.

The zero-potential-vorticity jet is particularly simple. Let the velocity (or speed) of the incoming jet be  $S(\eta)$ , where  $\eta$  is the cross-stream direction. Figure 2 shows the coordinates. The velocity profile of the jet is governed by the zero-potential-vorticity relation

$$\frac{\partial S}{\partial \eta} = -f,$$

which integrates to

$$S = -f\eta + c. \quad (3.1)$$

In the coordinate system used in figure 2,  $S = 0$  at  $\eta = 0$ , so  $c = 0$ . The height  $h$  is found using (2.1*b*) by substituting  $S$  and  $\eta$  for  $v$  and  $x$  and assuming  $u = u_y = 0$ . The resulting equation is geostrophic (as are all the jets entering or leaving the control volume) and is

$$fS = g' \frac{\partial h}{\partial \eta}.$$

Using (3.1) and integrating,

$$h = H - \frac{f^2 \eta^2}{2g'}, \quad (3.2)$$

where  $H$ , the constant of integration, is the depth of the stagnant fluid. The jet is of width

$$\eta_0 = \left( \frac{2g'H}{f^2} \right)^{\frac{1}{2}}, \quad (3.3)$$

which is the Rossby adjustment scale. We must find the contribution of  $S$  and  $h$  to the second integral in (2.6), is an integration over  $x$ ; thus  $S$  must be divided into its  $u$  and  $v$  components which must be expressed as functions of  $x$ .

The trigonometric transform between  $x$  and  $\eta$  is

$$\eta = x \cos \theta, \tag{3.4}$$

and the velocity distribution in the  $x$ - and  $y$ -directions is related to (3.1) by

$$u = -S \sin \theta = fx \cos \theta \sin \theta, \tag{3.5}$$

$$v = S \cos \theta = -fx \cos^2 \theta. \tag{3.6}$$

Since potential vorticity is conserved by the fluid and the currents are geostrophic, the velocity and depth profiles are uniquely determined. For the alongshore currents, the sequence of calculations to establish the velocity and depth distribution of  $u$  and  $h$  at  $x = \pm L$  will be analogous to those which led to (3.1)–(3.3). Thus the velocity and depth distributions are respectively linear and parabolic as before but, of course,  $u$  and  $h$  vary in  $y$  rather than  $\eta$ . The form of the velocity and depth profiles are the same as (3.1) and (3.2), but the constants of integration must be determined. Finally, since volume flux is conserved, depth  $h$  at the wall is the same at  $x = \pm L$ . This is needed to determine the constants.

The situation is summarized in figure 3, which shows the depth and velocity profiles of the offshore entrance section AB, and the left- and right-hand sections AC and BD respectively. The most important point is that *the velocity and height profiles are unchanged as the fluid leaves the control volume at  $x = \pm L$ . However, the fluid is split at the dividing streamline so that a jet of width  $\alpha$  exits to the left,  $\gamma$  to the right, where  $\alpha + \gamma = \eta_0$ . Our task is to determine  $\alpha$  (or  $\gamma$ ).*

To do this it is convenient to write the velocity at  $x = \pm L$  as

$$u = f(y + \gamma), \tag{3.7}$$

$$h = H - \frac{f^2(y + \gamma)^2}{2g'}, \tag{3.8}$$

where  $-\gamma > y > 0$ .

The velocity and height at  $x = -L$  is

$$u = f(y - \gamma), \tag{3.9}$$

$$h = H - \frac{f^2(y - \gamma)^2}{2g'} \tag{3.10}$$

at  $-\alpha < y < 0$ . At  $y = -\alpha = (\gamma - \eta_0)$ ,  $u = f\eta_0$  and  $h = 0$ . At  $y = 0$ , (3.9) and (3.10) have magnitudes equal to (3.7) and (3.8) respectively, but the velocities have opposite sign. Equations (3.1), (3.9) and (3.10) are, of course, consequences of the fact that volume flux into the volume must leave on both sides of the dividing streamline. The solutions (3.2), (3.4) and (3.5)–(3.10) are all incorporated into (2.6) to yield the final integral statement of momentum conservation

$$\int_{-\gamma}^0 \left( H - \frac{f^2(y + \gamma)^2}{2g'} \right) f^2(y + \gamma)^2 dy - \int_{-\alpha}^0 \left( H - \frac{f^2(y - \gamma)^2}{2g'} \right) f^2(y - \gamma)^2 dy - \int_{-\eta_0/\cos \theta}^0 \left( H - \frac{f^2 x^2 \cos^2 \theta}{2g'} \right) (fx \cos \theta \sin \theta) (-fx \cos^2 \theta) dx = 0. \tag{3.11}$$

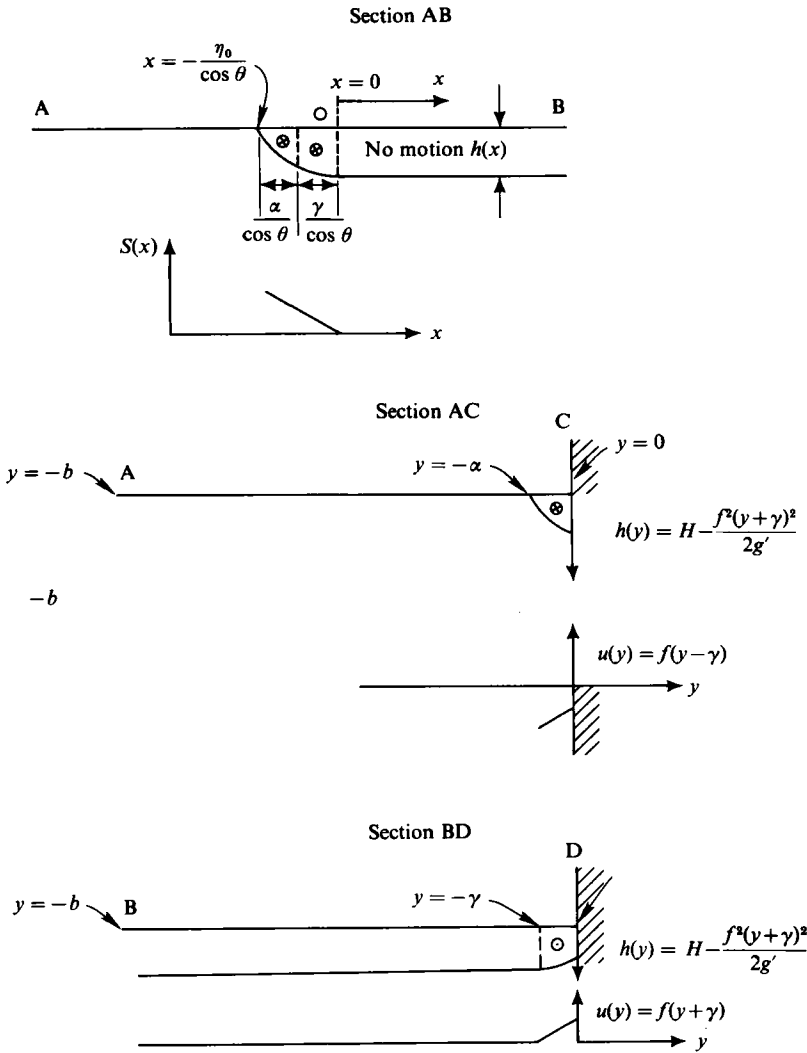


FIGURE 3. Sections AB (offshore), AC (left hand), and BD (right hand) from figure 2. The interface  $h$  between the jet fluid of density  $\rho$  and deep stagnant lower fluid of density  $\rho + \Delta\rho$  is shown. Velocity profiles for the offshore velocity  $S(x)$ , and alongshore velocity  $u(y)$  are also shown.

Our task is to solve for the unknown distance  $\gamma$  between the stagnation point and the zero-velocity point. This distance is a function of the incident angle  $\theta$ . The solution reveals the sizes of the currents exiting at  $x = \pm L$ . To solve for  $\gamma$ , it is convenient to recast (3.1) into a more convenient form by changing the variables as follows:  $y' = y + \gamma$ ,  $\tilde{y} = y - \gamma$  and  $\tilde{x} = x \cos \theta$ . Thus

$$\int_0^\gamma \left( H - \frac{f^2 y'^2}{2g'} \right) f^2 y'^2 dy' - \int_{-\eta_0}^{-\gamma} \left( H - \frac{f^2 \tilde{y}^2}{2g'} \right) f^2 \tilde{y}^2 d\tilde{y} + \int_{-\eta_0}^0 \sin \theta \left( H - \frac{f^2 \tilde{x}^2}{2g'} \right) (f^2 \tilde{x}^2) d\tilde{x} = 0. \quad (3.12)$$

All three integrals are of identical form, although they have different limits. By scaling the coordinates with the Rossby-deformation radius  $\eta_0$  (3.3) so that

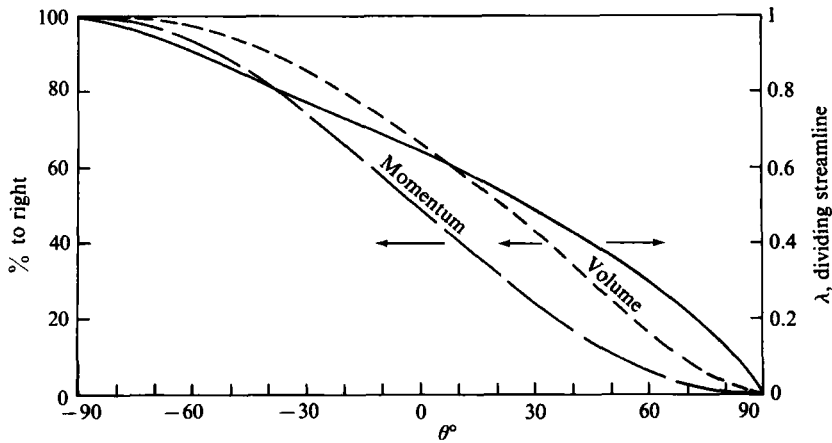


FIGURE 4. Results for a zero-potential-vorticity jet. The right ordinate is the dimensionless distance from the zero-velocity streamline to the stagnation point (see 3.13). The left ordinate is the percentage of momentum (from 3.15) and volume (from 3.17) fluxed to the right as a function of the incident angle of the jet.

$\eta_0 \beta = y' = \tilde{y} = \tilde{x}$ , the general problem can be reduced to

$$\int_0^\lambda (1 - \beta^2) \beta^2 d\beta - \int_\lambda^1 (1 - \beta^2) \beta^2 d\beta + \sin \theta \int_{-1}^0 (1 - \beta^2) \beta^2 d\beta = 0, \quad (3.13)$$

where  $\lambda = \gamma/\eta_0$  is the dimensionless distance of the stagnation-point streamline from the zero-velocity boundary. It is a very simple function of  $\theta$  as shown by the integral of (3.13) which is

$$\frac{2}{3}\lambda^3 - \frac{2}{5}\lambda^5 - \frac{2}{15} + \frac{2}{15} \sin \theta = 0. \quad (3.14)$$

The solution to (3.14) is shown in figure 4.  $\lambda$  varies continuously as the angle of incidence  $\theta$  changes. Note that the fluid always splits into two currents when  $\lambda$  is not equal to zero or one, which only happens for the extreme values of  $\theta = \pm 90^\circ$ .

One of the differences between this problem and the non-rotating-stagnation-point problem is that there is a lateral variation in velocity and depth in this jet. Thus the momentum-flux integrals

$$\int_0^\lambda (1 - \beta^2) \beta^2 d\beta \quad (3.15)$$

and 
$$\int_\lambda^1 (1 - \beta^2) \beta^2 d\beta \left( = \int_{-\lambda}^{-1} (1 - \beta^2) \beta^2 d\beta \right) \quad (3.16)$$

give the proportion of momentum which exits to the right and left respectively (the parenthetical equality is valid because the integral is odd). Since these are now only a function of  $\lambda$ , which is a unique function of  $\theta$  from (3.14), we can determine them. Equation (3.15) is presented in figure 4. The volume-flux integral to the right is easily found to be

$$\int_0^\lambda (1 - \beta^2) \beta d\beta = \frac{1}{2}\lambda^2 - \frac{1}{4}\lambda^4. \quad (3.17)$$

When it is normalized by the total scaled volume flux into the control volume, which is

$$\int_0^1 (1 - \beta^2) \beta d\beta = \frac{1}{4}, \quad (3.18)$$

the percentage of fluid going to the right as a function of  $\lambda(\theta)$  can be determined. This is also shown in figure 4. Generally a substantial amount of fluid goes to the right. For example, when the jet is tangential to the wall so that  $\theta = 0$ , more than 65% of the water goes to the right and less than 35% to the left.

#### 4. A constant-potential-vorticity jet

The above considerations can be extended to the case of a current of any known potential-vorticity distribution with little change as follows. The velocity and height distributions [the equivalents of (3.1) and (3.2)] are calculated for the offshore and coastal sections. The equivalent of the momentum-flux integral, (3.13), is found, the three integrals for momentum flux are calculated, and the equivalent to  $\lambda$  as a function of  $\theta$  is determined. Note that the momentum flux is the velocity squared times the height and is zero at both endpoints, since velocity is zero at one endpoint and height is zero at the other. The momentum flux has a maximum somewhere in the middle, at least for 'simple', i.e. unidirectional, currents. Therefore, the only way to get a current all to the right or left is to have  $\theta = \pm 90^\circ$ .

Jets of constant potential vorticity are produced by having fluid exit through a narrow passageway (Gill 1977; Nof & Olson 1983) from a basin of depth  $H$  and density  $\rho$  over a fluid of great depth and density  $\rho + \Delta\rho$ . They have been produced in laboratory experiments (Whitehead & Miller 1969; Stern *et al.* 1982; McClimans & Nilson 1982; McClimans & Green 1982; Griffiths & Hopfinger 1983). The jet shown in figure 1 has constant potential vorticity. A variety of oceanic surface currents may have approximately constant potential vorticity.

Theoretical solutions for constant-potential-vorticity currents are well known (Gill 1977; Stern *et al.* 1982; Nof & Olson 1983). The solution for the jet of constant potential vorticity offshore is found using the equation of constant potential vorticity

$$\frac{\partial S}{\partial \eta} - f = -\frac{fh}{H}, \quad (4.1)$$

and the geostrophic relation

$$fS = g' \frac{\partial h}{\partial \eta}. \quad (4.2)$$

Depth and velocity are

$$h = H(1 - e^{-\eta/\eta_0}), \quad (4.3)$$

and

$$S = \frac{g'}{f} \frac{H}{\eta_0} e^{-\eta/\eta_0}. \quad (4.4)$$

It is convenient to have the origin at the place where the front intersects the free surface. Thus the geometry is the same as in figure 2, except that the  $x$  origin is further to the left – at the solid line which denotes the edge of the front. The constant-potential-vorticity velocity profiles decay exponentially, there is nowhere with strictly zero motion. Thus the fine dashed line in figure 2 does not exist. We will call  $\delta$  the dimensionless distance from the edge of the front (i.e. the place where  $h = 0$ ) to the dividing streamline, using as a lengthscale the Rossby radius  $\eta_0$  appropriate for the constant-potential-vorticity problem. Thus  $\delta = \alpha/\eta_0$ , where

$$\eta_0 = \left( \frac{g'H}{f^2} \right)^{\frac{1}{2}}.$$

Relating  $S$ ,  $h$  and  $\eta$  to variables  $u$  and  $v$  at  $y = -b$ , and to  $u$  at  $x = \pm L$  is as

straightforward as it was in deriving (3.4)–(3.10). The velocity and height distributions are

$$u = \frac{g'H}{f\eta_0} \exp\left(\frac{y-\delta\eta_0}{\eta_0}\right) \quad (4.5)$$

$$h = H \left[ 1 - \exp\left(\frac{y-\delta\eta_0}{\eta_0}\right) \right] \quad \text{at } x \rightarrow +L \quad (4.6)$$

$$u = -\frac{g'H}{f\eta_0} \exp\left(\frac{-y+\delta\eta_0}{\eta_0}\right) \quad (4.7)$$

$$h = H \left[ 1 - \exp\left(\frac{-y+\delta\eta_0}{\eta_0}\right) \right] \quad \text{at } x \rightarrow -L \quad (4.8)$$

$$u = -\frac{g'}{f} \frac{H}{\eta_0} \exp\left(-\frac{x \cos \theta}{\eta_0}\right) \sin \theta \quad (4.9)$$

$$v = \frac{g'}{f} \frac{H}{\eta_0} \exp\left(-\frac{x \cos \theta}{\eta_0}\right) \cos \theta \quad (4.10)$$

$$h = H \left[ 1 - \exp\left(-\frac{x \cos \theta}{\eta_0}\right) \right] \quad \text{at } y \rightarrow b \quad (4.11)$$

and (2.6) reads

$$\begin{aligned} & \int_{-\infty}^0 \left[ 1 - \exp\left(\frac{y-\delta\eta_0}{\eta_0}\right) \right] \exp 2\left(\frac{y-\delta\eta_0}{\eta_0}\right) dy \\ & - \int_{-\delta\eta_0}^0 \left[ 1 - \exp\left(\frac{-y-\delta\eta_0}{\eta_0}\right) \right] \exp 2\left(\frac{-y-\delta\eta_0}{\eta_0}\right) dy \\ & - \sin \theta \cos \theta \int_0^{\infty} \left[ 1 - \exp\left(-\frac{x \cos \theta}{\eta_0}\right) \right] \exp\left(-\frac{2x \cos \theta}{\eta_0}\right) dx = 0. \end{aligned} \quad (4.12)$$

The structure of (4.12) is similar to (3.11), and the transformations

$$y' = \frac{y-\delta\eta_0}{\eta_0}, \quad \tilde{y} = \frac{y+\delta\eta_0}{\eta_0} \quad \text{and} \quad \bar{x} = \frac{x \cos \theta}{\eta_0}$$

simplify (4.12) to

$$\int_{-\infty}^{-\delta} (1 - e^{y'}) (e^{2y'}) dy' - \int_0^{\delta} (1 - e^{-\tilde{y}}) e^{-2\tilde{y}} d\tilde{y} + \sin \theta \int_0^{\infty} (1 - e^{-\bar{x}}) e^{-2\bar{x}} d\bar{x} = 0. \quad (4.13)$$

This integrates to

$$4e^{-3\delta} - 6e^{-2\delta} + 1 - \sin \theta = 0. \quad (4.14)$$

Figure 5 shows  $\delta$  as a function of  $\theta$ , and also shows the percentage of momentum flowing out of the right-hand side  $M_R$  given by the relation

$$M_R = 1 + 2e^{-3\delta} - 3e^{-2\delta}. \quad (4.15)$$

The volume flux out of the left-hand side  $Q_R$  is given by the relation

$$Q_R = 2e^{-\delta} - e^{-2\delta}. \quad (4.16)$$

A greater portion of the fluid goes to the right than with the zero-potential-vorticity jet. For instance, 75% goes to the right when  $\theta = 0$ .

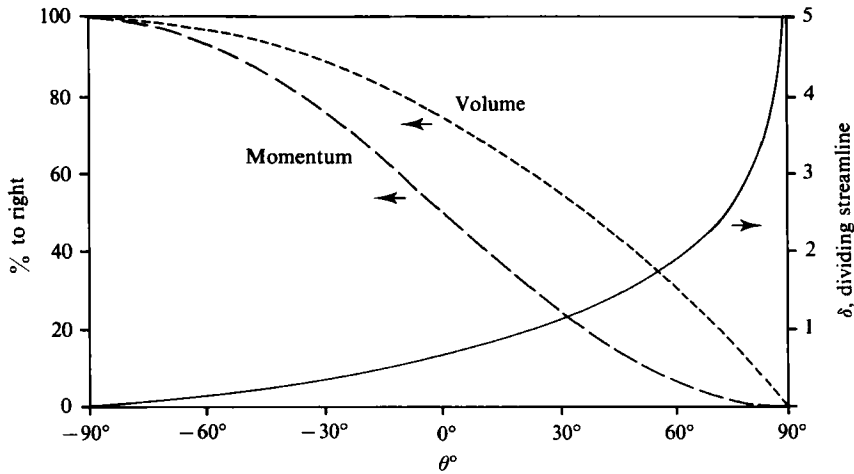


FIGURE 5. Similar to figure 4 except for a constant-potential-vorticity jet. The right ordinate is the dimensionless distance from the edge of the front to the stagnation point. The left ordinate is the percentage of momentum (from 4.15) and volume flux (from 4.16).

**5. Concluding remarks**

The normalized flux of momentum leaving the right-hand control volume is always equal to  $\frac{1}{2}(1 + \sin \theta)$ . This is implicit in (3.14) and (4.14). Thus, the momentum curves in figures 4 and 5 are the same. The quantity which determines the amount of volume flux to the left for any vorticity distribution is the ratio of the normalized volume-flux integral of the jet from zero to  $\delta$  to the normalized momentum flux, i.e.

$$f(\delta) = \frac{\int_0^\delta hv \, dy \int_0^\infty hv^2 \, dy}{\int_0^\delta hv^2 \, dy \int_0^\infty hv \, dy} \tag{5.1}$$

Since  $\int_0^\delta hv^2 \, d\eta / \int_0^\infty hv^2 \, d\eta$  is proportional to  $\frac{1}{2}(1 + \sin \theta)$ , (5.1) is

$$f(\delta) = \frac{2 \int_0^\delta hv \, dy}{\int_0^\infty hv \, dy (1 + \sin \theta)},$$

and its value gives the volume flux to the left as a function of  $\theta$ . Possibly this function can be calculated for actual ocean currents.

Figure 6 is an exercise in visualizing the distribution of volume flux and momentum flux of a constant-potential-vorticity jet. This shows normalized volume and momentum flux with their integrals as a function of the position from the outer edge of the jet. Since highest velocities occur at the outer edge of the jet, momentum flux is a maximum at approximately  $0.4\eta_0$ , while volume flux is a maximum at  $0.7\eta_0$ . In addition, from (4.13) we see that the momentum flux dies off as  $e^{-2\xi/\eta_0}$  for large  $\xi/\eta_0$  while volume flux dies off as  $e^{-\xi/\eta_0}$ . Thus, in general, the momentum flux is much more strongly concentrated near the edge of the jet than the volume flux and consequently, in the problem analysed here, there is a strong tendency for fluid to be deflected to

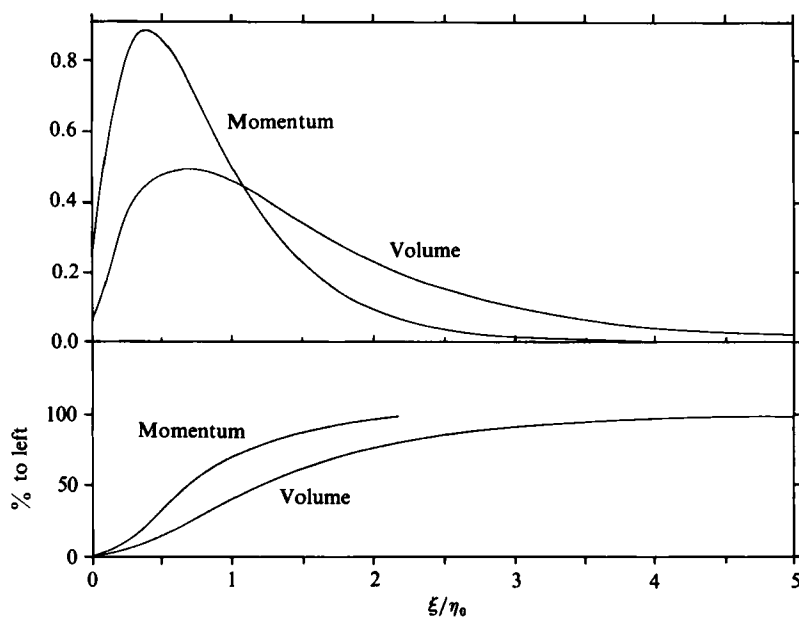


FIGURE 6. Momentum and volume flux (top), normalized to have an area of one, and their integrals (bottom) as a function of the dimensionless distance from the point where the front surfaces meet the wall. These are for a constant-potential-vorticity jet.

the right. In general, since the dynamically important momentum flux will more strongly affect the flows near the edge of the jet, this situation is conducive to blocking volume flux away from the edge of the front if such a jet goes along a curvy wall or if a free jet curves. Since the Gulf Stream is reported to have large amounts of constant-potential-vorticity water (Stommel 1966, pp. 109–110), these considerations may have some bearing on the formation of Gulf Stream rings.

Another interesting situation occurs when all the fluid is caused to go to the right or left at an angle other than  $\pm 90^\circ$ . This could happen if either velocity or height were zero somewhere in the middle of the jet or if the wall were a complicated shape, such as a deflector. This would violate the simple picture posed here, but it is by no means unrealistic.

If the wall had more complicated bottom topography, for instance if the wall were sloping in the vertical, the vorticity distribution of fluid in contact with a sloping wall would be different from the vorticity distribution offshore. Thus the velocity distribution would have changed. There is the possibility that the momentum flux along the wall might equal the momentum flux from offshore with all the fluid going either to the left or the right. Conversely, there may be cases where steady flows cannot exist because no jet incidence will be consistent with the momentum balance at the wall. Shore configurations that do this may strongly influence the path of boundary baroclinic jets and their behaviour next to coastlines.

The converse problem, of a jet steadily leaving a coast, may also be addressed with the integral method.

This idea was suggested by a stimulating lecture and discussion in Copenhagen, Denmark by Doron Nof describing the Nof & Olson (1983) paper. Joseph Pedlosky

provided important comments on the work for which thanks are given. Support was received from ONR Contract N00014-82-C-0019, NR 083-004. Woods Hole Oceanographic Institution Contribution Number 5651.

## REFERENCES

- BYE, J. A. T. & WHITEHEAD, J. A. 1975 A theoretical model of the flow in the mouth of Spencer Gulf, South Australia. *Estuar. Coast. Mar. Sci.* **3**, 477–481.
- CONLON, D. M. 1981 Dynamics of flow in the region of the Tsugaru Strait. *Tech. Rep. No. 312*, Coastal Studies Institute, Louisiana State University, Baton Rouge, LA, 62 pp.
- CONLON, D. M. 1982 On the outflow mode of the Tsugaru Warm Current. *La Mer* **20**, 60–64.
- GILL, A. E. 1977 The hydraulics of rotating-channel flow. *J. Fluid Mech.* **80**, 641–671.
- GRIFFITHS, R. W. & HOPFINGER, E. J. 1983 Gravity currents moving along a lateral boundary in a rotating fluid. *J. Fluid Mech.* **134**, 357–399.
- GRIFFITHS, R. W. & LINDEN, P. F. 1981 The stability of buoyancy-driven coastal currents. *Dyn. Atmos. Oceans* **5**, 281–306.
- INGEBRIGTSEN, J. 1979 Laboratory model of a coastal current. Thesis, Geophysics Institute, University of Bergen (In: Norwegian).
- KAWASAKI, Y. & SUGIMOTO, T. 1984 Experimental studies on the formation and degeneration processes of the Tsugaru Warm Gyre. In *Ocean Hydrodynamics of the Japan and East China Seas* (ed. T. Ichiye), pp. 225–238. Oceanog. Series, No. 39. Elsevier.
- KILLWORTH, P. D. & STERN, M. E. 1982 Instabilities on density-driven boundary currents and fronts. *Geophys. Astro. Fluid Dyn.* **22**, 1–28.
- MCCLIMANS, T. A. & GREEN, T. 1982 Phase speed and growth of whirls in a baroclinic coastal current. *River and Harbour Lab. Rep.* STF 60 A82108, Trondheim, Norway.
- MCCLIMANS, T. A. & NILSON, J. H. 1982 Whirls in the coastal current and their importance to the forecast of oil spills. *River and Harbour Lab. Rep.* STF 60 A82029, Trondheim, Norway.
- MORK, M. 1980 Formation and variability of a coastal front. In *Proc. 2nd Intl Symp. on Stratified Flows*, vol. 2, (ed. T. Carstens & T. A. McClimans), pp. 658–668. Tapir Press, Trondheim, Norway.
- NOF, D. 1978*a* On geostrophic adjustment in sea straits and wide estuaries: theory and laboratory experiments. Part I. One-layer system. *J. Phys. Oceanogr.* **8**, 690–702.
- NOF, D. 1978*b* On geostrophic adjustment in sea straits and wide estuaries: theory and laboratory experiments. Part II. Two-layer system. *J. Phys. Oceanogr.* **8**, 861–872.
- NOF, D. & OLSON, D. B. 1983 On the flow through broad gaps with application to the windward passage. *J. Phys. Oceanogr.* **30**, 1940–1956.
- PRANDTL, L. & TIETJENS, O. G. 1957 *Fundamentals of Hydro- and Aeromechanics*. (New Reproduction of 1934 Translated Edition 270 pp.), Dover.
- SAMBUCO, E. & WHITEHEAD, J. A. 1976 Hydraulic control by a wide weir in a rotating fluid. *J. Fluid Mech.* **73**, 521–528.
- SHEN, C. Y. 1981 The rotating hydraulics of the open channel flow between two basins. *J. Fluid Mech.* **122**, 161–188.
- STERN, M. E. 1974 Comment on rotating hydraulics. *Geophys. Fluid Dyn.* **6**, 127–130.
- STERN, M. E. 1980 Geostrophic fronts, bores, breaking and blocking waves. *J. Fluid Mech.* **99**, 687–703.
- STERN, M. E., WHITEHEAD, J. A. & HUA, B. L. 1982 The intrusion of a density current along a wall in a rotating fluid. *J. Fluid Mech.* **123**, 237–265.
- STOMMEL, H. 1966 *The Gulf Stream*. University of California Press, 248 pp.
- VINGER, A. & MCCLIMANS, T. A. 1980 Laboratory studies of baroclinic coastal currents along a straight, vertical coastline. *River and Harbour Lab. Rep.* STF 60 A80081, Trondheim, Norway.
- WHITEHEAD, J. A. 1985 A laboratory study of gyres and uplift near the Strait of Gibraltar. *J. Geophys. Res.*, in the press.
- WHITEHEAD, J. A., LEETMAA, A. & KNOX, R. A. 1974 Rotating hydraulics of strait and sill flows. *Geophys. Fluid Dyn.* **6**, 101–125.

- WHITEHEAD, J. A. & MILLER, A. R. 1979 Laboratory simulation of the gyre in the Alboran Sea. *J. Geophys. Res.* **84**, 3733–3742.
- WHITEHEAD, J. A. & PORTER, D. L. 1977 Axisymmetric critical withdrawal of a rotating fluid. *Dyn. Atmos. Oceans* **2**, 1–18.